ACS Sustainable Chemistry & Engineering

pubs.acs.org/journal/ascecg

Research Article

Case Study in Kraft Lignin Fractionation: "Structurally Purified" Lignin Fractions—The Role of Solvent H-Bonding Affinity

Reza Ebrahimi Majdar, Ali Ghasemian, Hossein Resalati, Ahmadreza Saraeian, Claudia Crestini,* and Heiko Lange*

Cite This: *ACS Sustainable Chem. Eng.* 2020, 8, 16803−16813

Read Online

ACCESS | Metrics & More | Article Recommendations | Supporting Information

ABSTRACT: Softwood kraft lignin **SKL** was fractionated using aprotic acetone and protic methanol to yield both previously reported "traditional" fractions and novel refined fractions thereof. Based on differences in mutual H-bonding affinities exerted by the solvents on one side and the OH group characteristics of the lignin oligo- and polymers on the other side, the 85% acetone-insoluble kraft lignin fraction **AIKL**, for example, could be further fractionated in 16% methanol-soluble and 67% methanol-insoluble parts. Sequential use of the two solvents practically resembled a refinement protocol that shed light on eventual "structural impurities" contained in the traditional fractions, which is not delineable easily in front of the background of a dominating spectroscopic image. Exploiting H-bonding characteristics offers a valid option for the facile generation of truly "structurally purified" lignin fractions. Acetone-insoluble, methanol-soluble **MSAIKL**, for example, exhibits 25% less aliphatic interunit bonding while being enriched in phenolic groups up to 25%, thus representing condensed, lower-molecular-weight structures with overall H-bond accepting character that was still contained in the overall larger-molecular-weight acetone-insoluble **AIKL**. More "polyphenylpropanoidic" parts practically free of condensed units, determining the overall structural picture of the unrefined lignins due to their overall abundance, are represented by the globally insoluble fractions like acetone-insoluble, methanol-insoluble **MIAIKL**. The original fractions and refined fractions generated based on targeting specific H-bonding affinities give a more homogeneous picture with respect to trends in glass transition temperatures, clearly indicating that T_g is dominated by actually both MW and nature of OH groups.

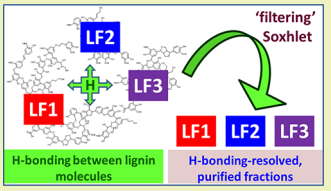

KEYWORDS: *softwood kraft lignin, H-bonding, fractionation, Soxhlet, membrane filtering, glass transition temperature*

INTRODUCTION

Polyphenolic renewable biomass, for example, in the form of lignins, could benefit much more from the growing trends of sustainability in general and substitution of fossil-based "traditional" active ingredients in every-day-life products in particular.[1−3] Especially, the use of technical lignins, however, is facing significant hurdles in the form of the structural and physical−chemical inhomogeneity of the lignin starting material that stems from differences in natural origins and emerges additionally from industrially feasible isolations. This inhomogeneity is found both in the molecular weight distribution and in underlying functional groups.[4]

Popular approaches to arrive at industrially more suitable polyphenolic starting materials on the basis of technical lignins are fractionation of lignins and/or their chemical derivatization. While the latter is purposefully targeting specific functional groups, fractionation usually aims at a separation of different molecular weight regimes within a technical lignin based on solubility differences. Fractionation of lignins has been investigated since the early 1950s,[5,6] and the field has seen recently numerous achievements, and some very recent reviews give more extensive overviews regarding lignin fractionations, highlighting also limitations.[7,8] Commonly used techniques, exemplary but not exclusively applied in the cited works, include sequential/fractional precipitations using either organic solvent systems[9,10] or pH variations in aqueous phases,[11] extractions using single solvents[12,13] or sequential applications of various solvents and[14−18] ultrafiltration.[19,20] While numerous studies on lignin fractionation do exist by now, only a few of them do actually present also sufficient amounts of structural data on each fraction that is needed for more direct comparisons (*vide infra*). Only very recently was presented an interesting approach that coupled solvent extraction with filtration and adsorption,[21] thus generating novel types of fractions for which some data were presented.

The fractionation of commercially available softwood kraft lignin (**SKL**), produced *via* the LignoBoost biorefinery process,[22] using an aprotic binary solvent system comprised of hexane as an apolar component and acetone as a polar component, was recently reported to yield fractions of different mean average molecular weights (Mn's) and narrow polydispersities.[9] A detailed study regarding the structural features of these **SKL** fractions revealed that the distribution of

Received: July 21, 2020
Revised: October 1, 2020
Published: November 3, 2020

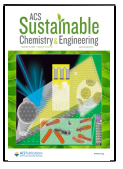

https://dx.doi.org/10.1021/acssuschemeng.0c05364
ACS Sustainable Chem. Eng. 2020, 8, 16803−16813

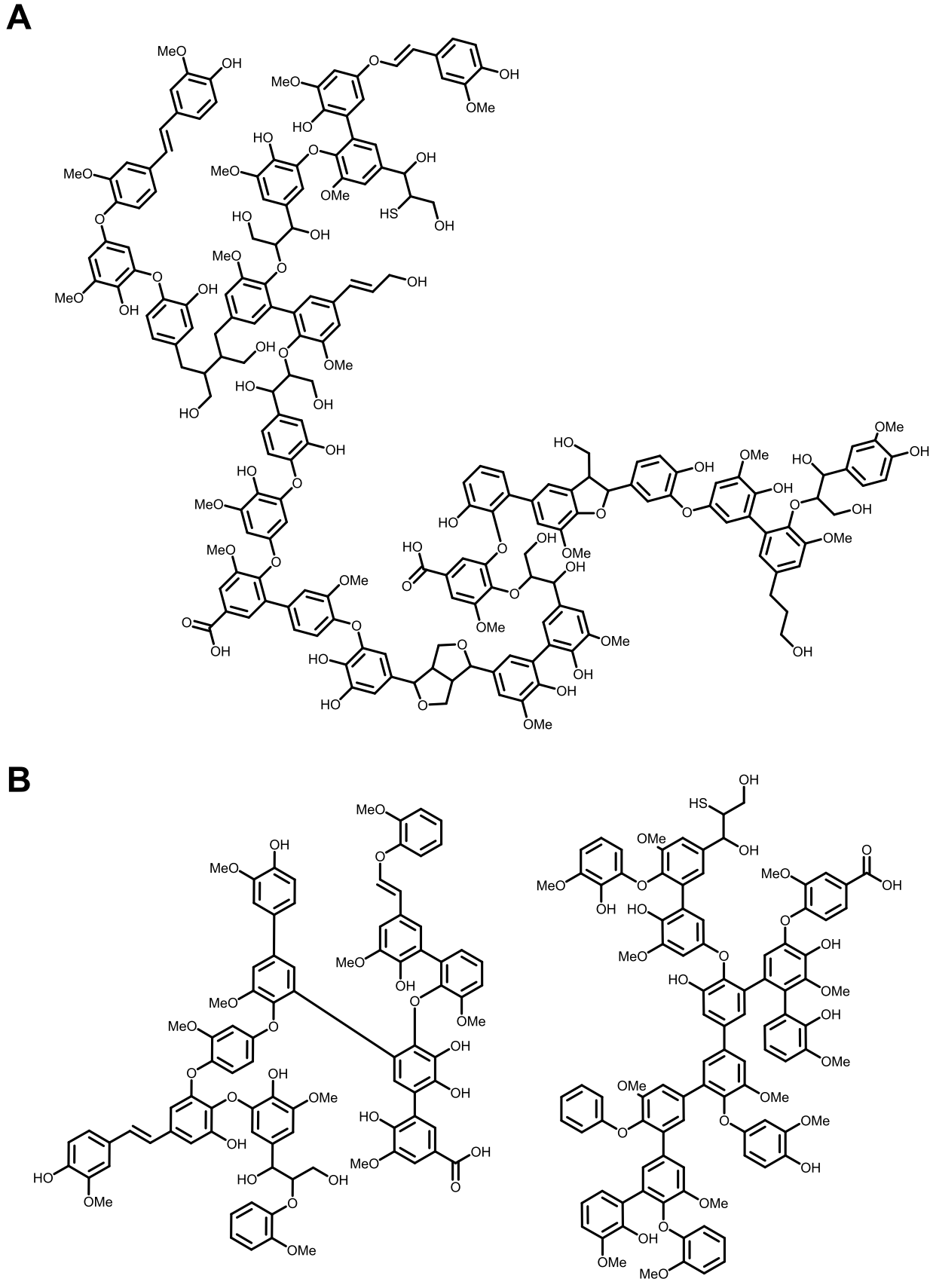

Figure 1. Structural features of softwood kraft lignin.[23] (A) Polymeric structures typical for the acetone-insoluble component; (B) condensed oligomeric structures typical for the acetone-soluble component.

https://dx.doi.org/10.1021/acssuschemeng.0c05364
ACS Sustainable Chem. Eng. 2020, 8, 16803−16813

functional groups and structural features is all but uniform across fractions. One basic finding was that fractions originating from the acetone-soluble part are mainly composed by condensed oligomeric polyphenols generated by repolymerization of monomeric fragments released during pulping and lacking the typical lignin propanoid side chain (Figure 1B). On the contrary, the acetone-insoluble component of **SKL** is mainly constituted by higher-molecular-weight lignin-like residues still containing significant amounts of propanoid side chains and typical lignin interunit bondings (Figure 1A).[23] Given these still rather general insights, the need for a lignin fractionation/purification strategy toward the isolation of structurally eventually even more homogeneous—in perspective, pure—kraft lignin components and an understanding of their physical properties arises. We became thus interested in developing fractionation processes that would holistically target not only homogeneous molecular weight distribution and the presence and amount of specific functional groups but also related H-bonding affinities in lignin components since they additionally strongly affect the associated tertiary structure of lignin oligomers and polymers.

Our strategy was not to repeat or just vary the various reported approaches based on sequences of solvent extractions following ordering schemes like Hanson solubility parameters[24] but to have a rational approach toward understanding lignin fractionation in the presence of solvents exhibiting different H-bonding characteristics and thus discriminating not only on the base of their polarity and dipole moment but also from their specific influence on the tertiary structure of lignin components. This approach recently yielded interesting and unexpected results in the case of organosolv wheat straw lignin.[17] The study was hence focused on sequential fractionation of **SKL** using solvents with identical polarity and comparable dipole moments but exhibiting a different H-boding character and dipole moment, such as acetone and methanol. Aiming at understanding also to what extent the molecular weight characteristics observed so far for fractions generated by sequential solvent washes are connected to the delineated structural features, an additional molecular weight targeting refinement method was introduced, replacing the conventional cellulose thimble of the Soxhlet setup by a dialysis bag made of regenerated cellulose exhibiting a defined molecular weight cut-off.

EXPERIMENTAL SECTION

General Procedure. Softwood kraft lignin **SKL** was produced *via* the LignoBoost process[22] by Stora Enso, Kotka, Finland; before use, **SKL** was kept at 40 °C in an oven until constant weight was obtained. Solvents in appropriate grades were purchased from Sigma-Aldrich and used as received if not stated otherwise. Dialysis filter tubes with 1−1.5 kDa cut-off made of regenerated cellulose were purchased from Spectrum Europe B.V., Breda, Netherlands.

Soxhlet Fractionation of SKL. Typically, 10 g of **SKL** or already derived fractions thereof was placed in a cellulose thimble or dialysis bag made from regenerated cellulose inside a Soxhlet extractor. The solvent chosen for the respective extraction step, typically 125 mL, was placed in a round-bottom flask that was heated by an oil bath. The solvent was brought to reflux and liquid solid extractions were continued until the solvent exiting at the end of an extraction cycle was colorless. Lignin fractions were isolated by drying the thimble and removing the solvent from the liquid fraction *in vacuo*. Final drying was achieved by placing the samples in an oven at 40 °C until constant weight was obtained.

Gel Permeation Chromatographic Analyses. For gel permeation chromatography (GPC), approximately 2−3 mg of lignin was dissolved in HPLC-grade dimethyl sulfoxide (DMSO) (Chromasolv, Sigma-Aldrich) containing 0.1% (m/v) lithium chloride (LiCl). A Shimadzu instrument was used, consisting of a controller unit (CBM-20A), pumping unit (LC 20AT), degasser (DGU-20A3), column oven (CTO-20 AC), diode array detector (SPD-M20A), and refractive index detector (RID-10A), and controlled by Shimadzu LabSolutions (version 5.42 SP3). For separation, a PLgel 5 μm MiniMIX-C column (Agilent, 250 × 4.6 mm) was eluted at 70 °C at 0.25 mL min^{-1} flow rate with DMSO containing 0.1% lithium chloride for 20 min. Standard calibration was performed with polystyrene sulfonate standards (Sigma-Aldrich; MW range, 0.43−2.60 × 10^6 g mol^{-1}) in acid form; lower calibration limits were verified by the use of monomeric and dimeric lignin models. Final analyses of each sample were performed using the intensities of the UV signal at λ = 280 nm employing a tailor-made MS Excel-based table calculation, in which the number-average molecular weight (Mn) and weight-average molecular weight (Mw) were calculated based on the measured absorption (in a.u.) at a given time (min) after baseline correction as described before.[25]

Quantitative ^{31}P NMR Analysis. A procedure similar to the one originally published and previously applied was used.[26,27] Approximately 30 mg of the lignin was accurately weighed in a volumetric flask and suspended in 400 μL of a solvent mixture of pyridine and deuterated chloroform ($CDCl_3$) (1.6:1, v/v), the above-prepared solvent solution. One hundred microliters of the internal standard solution, *i.e.*, cholesterol at a concentration of 0.1 M in the aforementioned NMR solvent mixture, was added. Fifty milligrams of Cr(III) acetyl acetonate was added as a relaxation agent to this solution, followed by 100 μL of 2-chloro-4,4,5,5-tetramethyl-1,3,2-dioxa-phospholane (Cl-TMDP). After stirring for 120 min at ambient temperature, the ^{31}P NMR spectra were recorded on a Bruker 400 MHz or Bruker 700 MHz NMR spectrometer controlled by TopSpin software using an inverse gated decoupling technique in the pulse sequence, with the probe temperature set to 20 °C. The maximum standard deviation of the reported data is 0.02 mmol g^{-1}, while the maximum standard error is 0.01 mmol g^{-1}.[26,28] NMR data were processed with MestreNova (version 8.1.1, Mestrelab Research).

^{1}H−^{13}C HSQC Analysis. Samples of around 50 mg were dissolved in 600 μL of DMSO-d_6 (providing NMR sample solutions with concentrations of around 83 mg/mL); chromium acetyl acetonate was added as a spin-relaxing agent at a final concentration of ca. 1.5−1.75 mg/mL. The HSQC spectra were recorded at 27 °C on a Bruker 400 MHz instrument equipped with TopSpin 2.1 software. The spectra were referenced to the residual signals of DMSO-d_6 (2.49 ppm for ^{1}H and 39.5 ppm for ^{13}C spectra). The ^{1}H−^{13}C HSQC spectra were obtained using the standard Bruker pulse program (hsqcegtpsisp2) with standardized numbers of scans (2048 (1H)/512 (13C). NMR data were processed with MestreNova (version 8.1.1, Mestrelab Research).

Differential Scanning Calorimetry (DSC). Differential scanning calorimetry was performed using a Mettler Toledo DSC/TGA 1 calorimeter or Mettler Toledo DSC 820 calorimeter. Typical sample amounts of around 4−6 mg were exactly weighted in 40 μL aluminum pans, which were closed with a lid that was centrally punctured to prevent pressure build-up. The following optimized temperature sequence was applied on all samples under a nitrogen atmosphere (50 mL min^{-1}) if not stated otherwise: 25 °C to 105 °C to 25 °C to 450 °C at a rate of 10 °C/min. Analysis was performed using Mettler Toledo Star1 software. Experiments were run in duplicate or triplicate if not stated otherwise.

RESULTS AND DISCUSSION

Previously reported fractionation approaches by solvent dissolution are based on the use of solvent batches to dissolve specific lignin fractions, as briefly indicated above. This approach intrinsically suffers from saturation bias. To avoid eventual issues bound to uncomplete dissolution, **SKL** was thus fractionated by exhaustive extractions in a Soxhlet setup using acetone as a H-bond accepting aprotic polar component

https://dx.doi.org/10.1021/acssuschemeng.0c05364
ACS Sustainable Chem. Eng. 2020, 8, 16803−16813

Scheme 1. Flow of Iterative Soxhlet-Based Fractionation of Softwood Kraft Lignin (SKL)[a]

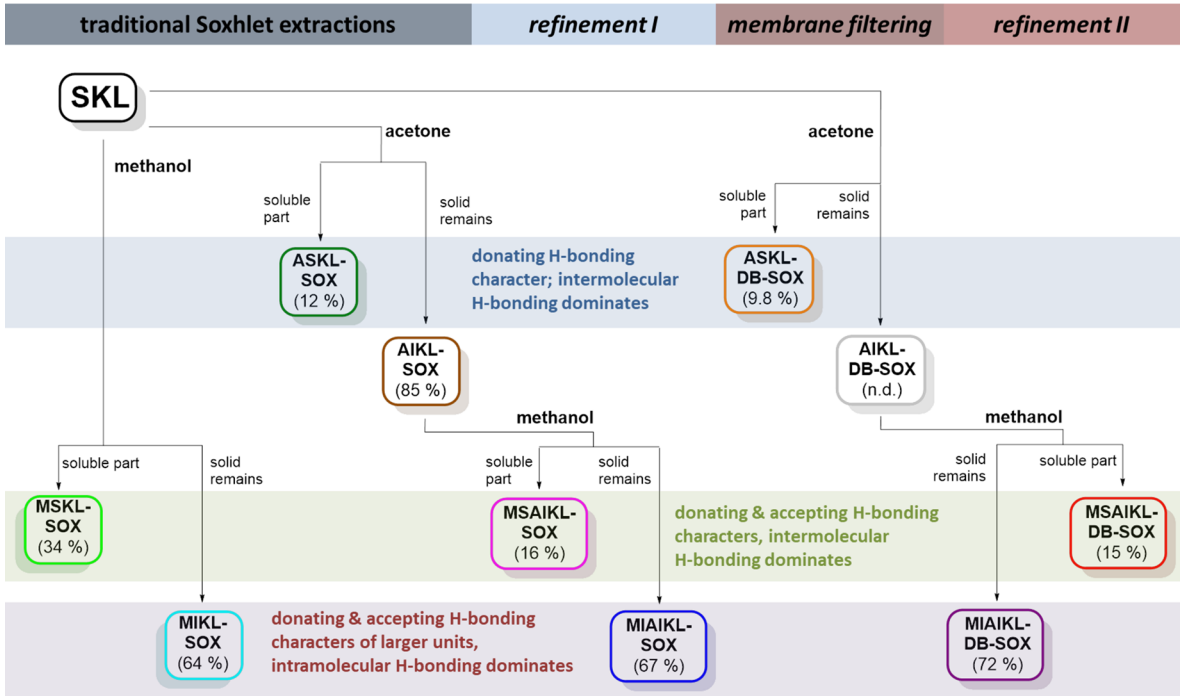

[a]Missing percentages indicate material loss due to the impossibility of isolating all the materials without contamination.

and methanol as a protic polar solvent capable of acting both as donor and acceptor in H-bonding, respectively. The two solvents were applied alone and in sequence but never in the form of binary systems. We hypothesized that differences in H-bonding affinities could be mainly targeted in the form of H-bond accepting and H-bond donating characteristics of especially exposed end groups, which in turn would reflect certain structural features.

To implement an element of additional control over molecular weight features, Soxhlet extraction was facultatively coupled to a membrane filtering process by simply using a dialysis bag instead of the traditional cellulose thimble. Scheme 1 illustrates the overall fractionation system, which can be divided in a traditional Soxhlet-based fraction, a membrane filtering process, and two refinements of the aforementioned steps. All resulting fractions were structurally analyzed and studied regarding their glass transition temperatures as a function of revealed structural features.

Softwood Kraft Lignin Fractionation. **SKL** was at first fractionated in a typical Soxhlet extractor equipped with a traditional cellulose thimble starting with exhaustive extraction of solid **SKL** with acetone (Scheme 1). Removal of solvents from the extractives and recovering of the solid residues from the thimble yielded 12% of Soxhlet-derived acetone-soluble softwood kraft lignin, *i.e.*, **ASKL-SOX**, and 85% of Soxhlet-derived acetone-insoluble softwood kraft lignin, *i.e.*, **AIKL-SOX**, after drying at 40 °C in a vacuum oven. The weight loss of 3% represents parts of the lignin that could not be recovered from the rough surface of the thimble without risking a cellulose contamination of the isolated lignin.

In a similar fashion, 34% of methanol-soluble softwood kraft lignin (**MSKL-SOX**) and 64% of methanol-insoluble softwood kraft lignin (**MIKL-SOX**) were obtained (Scheme 1); weight loss is again due to the material being not entirely recoverable without risking sample contamination.

The literature suggests that methanol is able to dissolve low-molecular-weight fractions from lignin; such fractions, however, were not reported to be of condensed nature as low-molecular-weight acetone fractions. To delineate to what extent such methanol-soluble low-molecular-weight species are still present in the acetone-insoluble fraction, **AIKL-SOX** was further refined in a Soxhlet extractor using methanol (refinement I, Scheme 1). Novel fractions **MSAIKL-SOX** and **MIAIKL-SOX** were obtained in 19 and 79% yields, respectively, corresponding to 16 and 67% of the overall lignin used.

In an attempt to confirm that the **ASKL** fraction is mainly comprised of low molecular weight, rather condensed oligomers in the range of 1−1.5 kDa as suggested by seminal publications,[23,29] a physical means of polymer size control was implemented in the Soxhlet-based extraction process. **SKL** was loaded in a dialysis tube, presenting a membrane filter of regenerated cellulose with a molecular weight cut-off of 1−1.5 kDa. This tube was placed in a conventional Soxhlet extractor, replacing the cellulose thimble. No degradation of the dialysis tube was observed during the extraction process (membrane filtering, Scheme 1) that allowed isolation of approximately 10% of acetone-soluble, dialysis bag-filtered kraft lignin, *i.e.*, **ASKL-DB-SOX**. Residues remaining in the dialysis bag, *i.e.*, **AIKL-DB-SOX**, were directly submitted to a refinement *via* extraction with methanol, in analogy to the first methanol refinement, following the rationale above for **MSAIKL-SOX** (refinement II, Scheme 1). Oven-dried **MSAIKL-DB-SOX** and **MIAIKL-DB-SOX** fractions were isolated in 13 and 72% mass returns, respectively.

Fractions were analyzed for molecular mass characteristics using gel permeation chromatography as well as for structural insights using quantitative ^{31}P NMR spectroscopy and semiquantitative ^{1}H−^{13}C HSQC measurements.

https://dx.doi.org/10.1021/acssuschemeng.0c05364
ACS Sustainable Chem. Eng. 2020, 8, 16803−16813

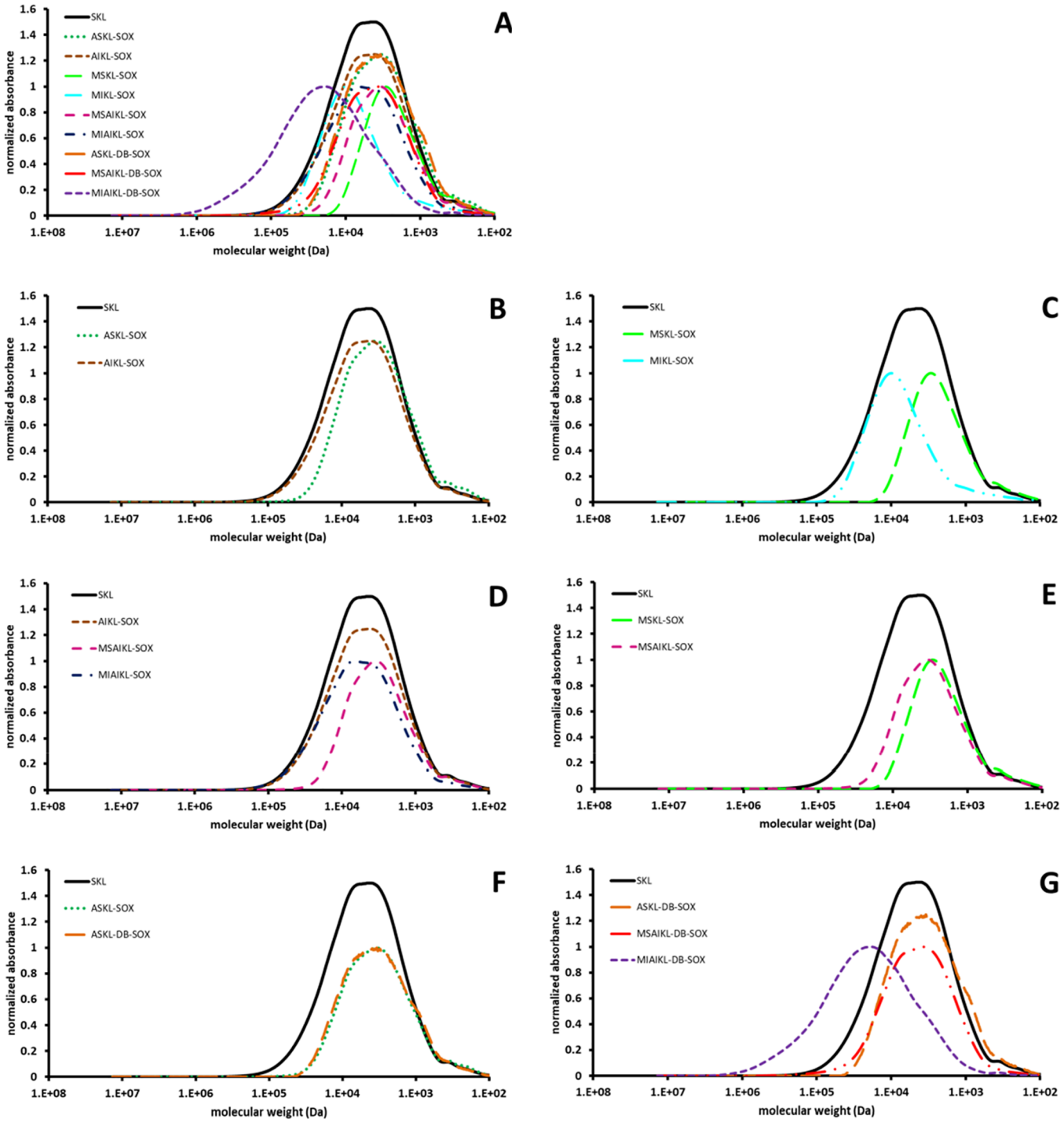

Figure 2. GPC analyses of softwood kraft lignin (**SKL**) and Soxhlet-derived fractions thereof: (A) comparison of all obtained fractions; (B) pure acetone-derived fractions; (C) pure methanol-derived fractions; (D) **AIKL-SOX** and methanol fractions derived thereof; (E) methanol-soluble fractions; (F) **ASKL-SOX** and **ASKL-DB-SOX**; (G) comparison of **DB-SOX** fractions. Corresponding molecular weight features are listed in Table 1.

Molecular Weight Characteristics of SKL Fractions. Gel permeation chromatography was carried out in DMSO to assure the solubility of samples and to skip chemical functionalization prior to the analysis to avoid possible structural changes eventually caused during this procedure.[30] Figure 2 shows comparisons of GPC traces; mean-average molecular weights are reported in Table 1.

ASKL-SOX and **AIKL-SOX** differ in their molecular mass characteristics (Mn of 1450 Da *vs* 2000 Da, respectively) as expected, with acetone-insoluble **AIKL-SOX** numerically exhibiting a higher mean-average molecular weight (Figure 2B and Table 1, entries 2 and 3). **ASKL-SOX** exhibits slightly better polydispersity than parent **SKL** or **AIKL**. A similar trend is observed for the methanol-based Soxhlet fractionation (Figure 2C and Table 1, entries 4 and 5). **MSKL-SOX** is of lower number-average molecular weight (Mn = 1100 Da) than **MIKL-SOX** that displays a Mn of 1900 Da. These findings are

https://dx.doi.org/10.1021/acssuschemeng.0c05364
ACS Sustainable Chem. Eng. 2020, 8, 16803−16813

Table 1. Molecular Weight Characteristics and OH Group Contents (*via* Quantitative ^{31}P NMR after *In Situ* Phosphitylation Using 2-Chloro-4,4,5,5-tetramethyl-1,3,2-dioxaphospholane) Obtained for SKL and Solubility-Based Fractions Thereof

			aromatic OH [mmol/g]					
sample	Mn [Da] (PD)[a]	aliph. OH [mmol/g]	cond. OH/guaiacyl OH/*p*-OH	total	acidic OH [mmol/g]	total OH [mmol/g]	aromatic OH/ aliphatic OH	T_g [°C][b]
SKL	2100 (3.9)	2.07	1.86/2.09/0.24	4.19	0.44	6.70	2.0	138
ASKL-SOX	1450 (3.2)	1.59	2.07/2.64/0.32	5.03	0.58	7.20	3.2	118
AIKL-SOX	2000 (3.9)	1.72	1.68/1.77/0.24	3.69	0.38	5.79	2.1	146
MSKL-SOX	1100 (2.7)	2.08	2.02/2.48/0.33	4.83	0.47	7.38	2.3	170
MIKL-SOX	1900 (5.4)	1.95	1.87/1.77/0.30	3.94	0.33	6.22	2.0	175
MSAIKL-SOX	1550 (2.8)	1.96	1.87/2.37/0.24	4.48	0.32	6.76	2.3	173
MIAIKL-SOX	2300 (4.1)	2.08	1.92/1.95/0.19	4.06	0.20	6.34	2.0	174
ASKL-DB-SOX	1600 (3.0)	1.57	2.06/2.38/0.25	4.69	0.37	6.63	3.0	112
MSAIKL-DB-SOX	2100 (3.4)	1.63	1.84/2.00/0.24	4.08	0.30	6.01	2.5	131
MIAIKL-DB-SOX	5600 (8.2)	2.34	1.43/1.26/0.18	2.87	0.15	5.36	1.2	169

[a]Polydispersity index. [b]As determined by DSC analysis. In the case of multiple detectable glass transition temperatures, the lowest one is listed here.

generally comparable to results reported for the fractional dissolution of **SKL** in methanol.[12]

With Mn = 1550 Da, **MSAIKL-SOX** showed a significantly lower mean-average molecular weight than the parent **AIKL-SOX** but a higher Mn than **MSKL-SOX**, thus indicating that methanol is able to extract the low-molecular-weight fraction of **AIKL-SOX**. **MSAIKL-SOX** thus has a comparable Mn to **ASKL-SOX**. Residual **MIAIKL-SOX** exhibited a considerably higher molecular weight (Mn) of 2300 Da (Figure 2D and Table 1, entries 6 and 7). These results indicate that a simple acetone extraction is not sufficient to fully isolate low-molecular-weight structures from high-MW fractions since **AIKL-SOX** obviously still comprised low-MW fractions that were only soluble in methanol. The fact that these fractions are soluble only in a protic solvent can be interpreted as a hint that these exhibit different structural features than **ASKL**. Comparing the GPC traces of **MSAIKL-SOX** with **MSKL-SOX** evidences that the pure methanol fractionation is of overall lower mean-average molecular weight (Figure 2E). As the below-discussed structural analysis showed, **MSKL-SOX** can be treated as a mix of oligomeric chains containing **SKL**-typical aliphatic moieties and oligomeric condensed structures.

ASKL-DB-SOX exhibits practically molecular weight data like **ASKL-SOX** (Figure 2F). **ASKL-SOX** can thus be considered to comprise oligomeric structures below the effective cut-off of the low MW dialysis tube, hence confirming previously published oligomer sizes of maximum 1500 Da.[23,29]

MSAIKL-DB-SOX and **MIAIKL-DB-SOX** differ more significantly in MW than the corresponding thimble fractions (Figure 2G) as could be expected in light of above-discussed findings. Interestingly, methanol-soluble **MSAIKL-DB-SOX** is of higher mean-average molecular weight and higher polydispersity than **MSAIKL-SOX**. The dialysis membrane must thus have effectively held back typically acetone-soluble oligomers of higher molecular weight, which are also soluble in MeOH and adopt a different hydrodynamic volume in the protic environment, allowing passing of the membrane filter as part of the methanol-soluble dialysis-bag fraction. **MSAIKL-DB-SOX** was thus expected to show a slightly different OH group content.

Structural Features of SKL Fractions. Structural analysis started using quantitative ^{31}P NMR spectroscopy to allow for identification of differences in terms of hydroxyl group contents between various fractions. Results are summarized in Table 1. In agreement with the trends seen for solvent-precipitated fractions of **SKL** reported before,[23] the acetone-soluble fractions show a decrease in aliphatic OH group content and increase in phenolic OH groups. Acetone-insoluble fractions, on the other hand, show more similar distributions of OH groups compared to the parent **SKL**. Combined findings of the GPC analysis and ^{31}P NMR analysis show that the Soxhlet-derived acetone-soluble **ASKL-SOX** fraction is similar to the acetone-soluble fraction, *i.e.*, the nonprecipitating fraction obtained before.[9,23] The acetone-insoluble **AIKL** fraction, on the contrary, was found to be eventually comprised of larger polymers that are less condensed and containing a higher degree of aliphatic moieties.[23] Accordingly, the ratio between aliphatic OH groups and phenolic OH groups is significantly different for **ASKL-SOX** and **AIKL-SOX**, *i.e.*, 3.2 *vs* 2.1, respectively.

In the case of **MSKL-SOX** and **MIKL-SOX**, the soluble fraction is overall richer in OH groups, exhibiting especially a higher absolute phenol content compared to the insoluble fraction. Interestingly, however, the ratio between aliphatic OH groups and phenolic OH groups is of about 1:2 for both fractions; significant differences for this couple are only found in the acidic OH group content (Table 1).

When refining acetone-insoluble kraft lignin fractions using methanol, significant differences between **MSAIKL-SOX** and **MIAIKL-SOX** are seen, especially in a high content of guaiacyl-type phenolic OH groups that contribute to a general higher prevalence of phenolic OH in the case of **MSAIKL-SOX**. Aliphatic OH group content shows a contrary trend in comparison to the methanol-only fractions, being slightly elevated in **MIAIKL-SOX**. Generally, differences between fractions are less pronounced than in the case of sole acetone or sole methanol fractions (Table 1), in analogy to findings regarding the molecular weights.

When the thimble is substituted with the dialysis membrane for the acetone extraction, generated **ASKL-DB-SOX** is found to contain ca. 8% less OH groups in total compared to **ASKL-SOX** with the loss mainly being attributable to losses in carboxylic OH groups (36%) and guaiacyl OH groups (10%), respectively.

MSAIKL-DB-SOX and **MIAIKL-DB-SOX**, obtained as refinement products in the membrane filtration of non-isolated **AIKL-DB-SOX** with methanol, exhibit trends for end groups similar to those observed for methanol extraction of **AIKL-**

https://dx.doi.org/10.1021/acssuschemeng.0c05364
ACS Sustainable Chem. Eng. 2020, 8, 16803−16813

Table 2. Trends in Abundances of Interunit Bonding Motifs, Identified Based on Archival Literature,[31−33] in the Different SKL Fractions[b]

Bonding motif	δ ^{1}H (ppm)	δ ^{13}C (ppm)	signal difference to SKL [%]						
			ASKL-SOX	AIKL-SOX	MSKL-SOX	MIKL-SOX	ASKL-DB-SOX	MS-AIKL-SOX	MS-AIKL-DB-SOX
G-propanol	1.66	34.99	10.21	-3.40	9.36	-0.85	24.68	28.94	-1.28
Hγ in cinn-OH	4.1	62.04	-1.39	1.39	-26.39	-8.33	-8.33	1.39	0.00
Hα in β-*O*-4'	4.8	71.52	-19.23	-0.96	-21.15	0.96	-24.04	-14.42	2.88
Hβ in β-O-4' with α-C=O	7.45	111.41	34.38	2.08	47.92	-8.33	25.00	47.92	2.08
Hα in β-5'	5.5	87.11	-16.67	-3.33	-23.33	13.33	-20.00	-16.67	-10.00
Hα in β-β'	4.62	85.23	-14.29	0.00	-12.70	4.76	3.17	-15.87	15.87
Hα in epi-β-β'	4.3	87.27	-14.29	23.81	33.33	28.57	-57.14	23.81	38.10
BE / Hα' in epi-β-β'	4.76	81.64	-21.21	-30.30	-21.21	-9.09	-6.06	-15.15	-6.06
xylan		[a]	-67.14	42.33	-63.44	53.73	-107.75	-53.73	-40.19

[a]Values represent the average change of three signals with the following centers of shifts: δ ^{1}H/δ ^{13}C [ppm]: 3.06/72.97; 3.29/74.25; 3.52/75.84. [b]Numbers represent differences of abundances in percentages compared to the parent **SKL** on the basis of abundances normalized to the methoxy group abundance in each fraction. Significant differences (≥|7.5|) have been additionally color-coded.

SOX contained in a traditional cellulose thimble (Table 1). In both cases, the overall insoluble parts, *i.e.*, **MIAI** fractions, are enriched in aliphatic OH groups while exhibiting lower total OH group content. In the case of the methanol refinement of **AIKL**, these differences are, however, even more strongly pronounced (Table 1). **MSAIKL-DB-SOX** exhibits a similar ration of aliphatic to aromatic OH groups compared to **MSAIKL-SOX**, which results from a reduction of both aliphatic OH groups and guaiacyl-type phenolics. This could be interpreted, in connection with GPC data, as that less condensed, slightly larger oligomers, *i.e.*, oligomers containing more intact typical lignin side chains that are present in **MSAIKL-SOX**, can be retained using a means of filtering.

Interestingly, the ratio between aromatic and aliphatic OH groups is reduced in **MIAIKL-DB-SOX** in comparison to **MIAIKL-SOX** by approximately 15%. Together with the data from the GPC analyses, this suggests that **MIAIKL-DB-SOX** represents a fraction of truly polymeric lignin chains that exhibit a comparably low amount of phenolics as end groups while including less compromised aliphatic lignin motifs and hydroxylated alkyl residues as additional end groups; eventually, carbohydrate residues "pollute" this lignin fraction.[23,31]

The results by the ^{31}P NMR analysis suggest structural differences that were expected to be reflected also in detectable differences in the HSQC spectra of parent **SKL** and its various fractions. Using standardized acquisition parameters in terms of sample concentration and acquisition times, the qualitatively comparable HSQC spectra were obtained for soluble acetone-derived fractions **ASKL-SOX**, **AIKL-SOX**, and **ASKL-DB-SOX** as well as soluble methanol-derived fractions **MSKL-SOX**, **MIKL-SOX**, **MSAIKL-SOX**, and **MSAIKL-DB-SOX**; **MIAIKL-DB-SOX** was practically insoluble under analysis conditions.

While the quantitative ^{31}P NMR spectra reveal noticeable differences in OH groups in various fractions, the HSQC spectra appear surprisingly similar at a first glance, more visibly indicating just the fact that **ASKL-SOX**, **MSKL-SOX**, and **ASKL-DB-SOX** contain potentially extractable impurities in higher concentrations now, whereas typical xylan cross-peaks are evident only in **AIKL-SOX** and **MIKL-SOX** fractions.[23] To delineate eventually present, more subtle differences within the lignin structures themselves, selected signals indicative of characteristic lignin interbonding and terminal motifs have been normalized to the signal intensity of the methoxy groups for each fraction. Relative differences with respect to starting **SKL** are given in Table 2; underlying absolute data are listed in the Supporting Information.

ASKL-SOX is, with respect to the unfractionated parent lignin, depleted in "classical" interunit bonding motifs and enriched in α-oxidized β-aryl ethers and aliphatic end groups; **AIKL-SOX** is by and large similar in aliphatic interunit motifs compared to the parent **SKL** and furthermore enriched in xylan impurities (Table 2). These findings correspond to the ^{31}P NMR results for this fraction as reported in Table 1.

Analogous to **ASKL-SOX**, **MSKL-SOX** is depleted in aliphatic interunit bonding motifs and enriched in α-oxidized motifs while it is additionally poorer in unsaturated terminal motifs like cinnamyl alcohols. **MIKL-SOX** represents the expectable counterpart. Interestingly, sugar residues are contained solely in the insoluble fractions (E, Table 2), as indicated already by the ^{31}P NMR analysis.

When **AIKL-SOX** is additionally fractionated using methanol, **MSAIKL-SOX** shows the same enrichments as the methanol-soluble fraction that is obtained directly from **SKL**. Sugar residues enriched in **AIKL-SOX** remain in the insoluble phase, thus confirming the observation made for **MSKL-SOX**.

Just as in the ^{31}P NMR analysis, **ASKL-DB-SOX** shows also in the HSQC subtle differences to **ASKL-SOX**, with more aliphatic end groups, less enrichment in α-oxidized β-*O*-4′ and a loss in β-aryl ethers. Accumulative analysis correlates with ^{31}P NMR findings.

When **AIKL-DB-SOX** is additionally dialyzed with methanol in the Soxhlet setup, generated **MSAIKL-DB-SOX** is found to be different from corresponding **MSAIKL-SOX**, exhibiting a tendency to be especially enriched in native lignin interbonding motifs resinol and phenylcoumaran. This fraction is not enriched in saturated aliphatic end groups since these have been accumulated in the previously washed out **ASKL-DB-SOX** fraction. Data suggest that sugar residues are successfully

https://dx.doi.org/10.1021/acssuschemeng.0c05364
ACS Sustainable Chem. Eng. 2020, 8, 16803−16813

retained in the **MIAIKL-DB-SOX** fraction since sugars are retained in the insoluble part.

The observed distribution of functional groups both by ^{31}P NMR and HSQC analyses can be seen as a consequence of the intrinsic H-bonding characteristics of these groups.[34] In the acetone-soluble **ASKL-SOX** fraction, which is rich in phenolic OH groups and poor in aliphatic OH groups, an intermolecular donating H-bonding dominates. In the corresponding acetone-insoluble **AIKL-SOX** fraction, structures that exhibit mixed donating and accepting H-bonding characteristics remain. Nevertheless, some of these mixed-character species might undergo stronger intermolecular H-bonding than intramolecular H-bonding if a solvent is offered that can cope with this mixed character while being able to substitute/compete with the intramolecular H-bonding during solubilization. The **MSAIKL-SOX** fraction represents the "product" of such a H-bonding competition experiment: (i) it is low enough in molecular weight to be soluble in methanol; (ii) it represents functional groups exhibiting donating H-bonding characteristics like in **ASKL-SOX** but can act simultaneously very well as a H-bonding acceptor owing to a still relatively high amount of aromatic systems, *via* "H-π-bonding",[35] and owing to an ever more elevated presence of oxidized side chains, such as α-oxidized β-*O*-4′ motifs. The overall insoluble **MIAIKL-SOX** fraction does not display a single dominating H-bonding character, but its lignin molecules, relatively richer in aliphatic OH groups, employ most of their H-bonding capacity in intramolecular interactions.[34] Existing intermolecular H-bonding with other higher oligomeric or polymeric lignin molecules renders this fraction overall insoluble when applying H-bonding-based solvent systems.

MIAIKL-SOX can thus be seen as a fraction with a mixed but equilibrated H-bonding profile, while **ASKL-SOX** and **MSAIKL-SOX** together represent the fraction with homogenized H-bonding profiles that are dominated by the prevailing condensed character. When this separation is not good enough for applications that demand an even stricter differentiation between oligomeric condensed and polymeric phenylpropanoid characters, additional refinement is achieved by the implementation of a means of filtering in the otherwise unchanged process.

An aspect related to H-bonding is the generally observed accumulation of the aforementioned sugar residues, detectable in the form of xylanes, in the insoluble fractions. More interesting, however, is the delineable indication on the nature of the xylan residues in the kraft lignin under study, *i.e.*, on whether they are simply present as "pure" carbohydrate residues or in the form of lignin carbohydrate complexes (LCCs). Xylan residues have been postulated to be eventually linked to lignin oligo- and polymeric structures *via* benzyl ethers (**BEs**) as one form of commonly discussed LCC linkages. A cross-peak corresponding to the benzyl hydrogen is detectable in all fractions, *i.e.*, also in the fractions that are essentially free of carbohydrate-stemming cross-peaks (Table 2). The **BE**-characterizing signal has been reported to be overlapped with signals corresponding to epiresinol, *i.e.*, epi-β-β′ as a putative interunit bonding motif typical for kraft lignins.[31,36,37] The fact that the fractions show only variations in the **BE**/epi-β-β′ signal, but no complete disappearance together with the carbohydrate residues, thus allows for speculating that the kraft lignin under study contains epiresinol motifs. The fact that the signal is not unambiguously enriched in the sugar-containing, insoluble fractions could further be interpreted as that the sugars are by and large not present in the form of LCCs. Cross-peaks reported for other LCC motifs cannot be detected either in the parent **SKL** or in any of its fractions generated in this study, supporting this interpretation.

Placement of Novel Refined Fractions in the Existing Landscape of Kraft Lignin Fractions. Two studies obtained acetone-soluble fractions from a LignoBoost lignin in amounts of approximately 70%, submerging a certain amount of softwood **KL** in a defined volume of acetone. The soluble fraction was separated from the insoluble fraction after mechanical stirring the suspension and a vacuum filtration.[9,15] The reasons for the noticeable difference in the amount of isolated acetone-soluble **KL** to this study can thus be understood on the basis of the fundamental differences between the methods used for its formation. When using the Soxhlet setup, avoiding any form of physical forces that could influence solubilization, isolated yields of **ASKL-SOX** were repeatedly found to be within the reported 12 ± 3% yield. Comparable 14% for an acetone-soluble fraction was reported in a study using a different sequential solvent fractionation of a softwood **KL**.[16] The fractions generated by simple initial Soxhlet extraction using acetone, *i.e.*, **ASKL-SOX** and **AIKL-SOX**, structurally resemble fractions encountered before in the case of softwood kraft lignin in the form of fractions precipitated from acetone−hexane mixtures with high molar ratios of hexane and more directly corresponding acetone-insoluble fraction, respectively, as far as this can be stated analyzing the structural information in the cited reports and the not fully quantitative analysis performed in here for comparative structural discussion.[23]

In the case of the straightforward methanol fractionation, generated fractions **MSKL-SOX** and **MIKL-SOX** are by and large comparable in yield to a previously reported work on the fractionation of a kraft lignin.[12] Structurally, comparison indicates similar molecular weight trends on the basis of a very similar GPC method and rather similar distributions of OH groups revealed in both cases on the basis of quantitative ^{31}P NMR analysis.

The other fractions do not have direct correspondences in the archival literature as such and represent novel refined lignins exhibiting more narrowly accumulated, *i.e.*, "H-bonding resolved", structural features, leading eventually to more pronounced differences in interunit bonding motifs as discussed in the preceding dedicated paragraphs.

The low yields of especially the soluble fractions could be seen as a potential bottleneck with respect to plausible applications of the novel fractions. Such fractions, given their more defined structural features, are currently favored for and tested in truly higher value applications in functional cosmetics fields, for which smaller amounts are sufficient. To generate such smaller fractions on scale, the proposed approach can be coupled with a continuous fractionation approach based on fractional dissolution recently developed in our laboratories.[18]

Thermal Properties of Soxhlet-Derived SKL Fractions. The thermal properties of **SKL** fractions are expected to significantly differ, given that both mean-average molecular weights and functional group contents here, especially the ratio between phenolic and aliphatic OH groups, vary significantly between fractions. The glass transition temperatures (T_g's) obtained for various fractions by differential scanning calorimetry are listed in Table 1. For delineating eventual correlations, glass transition temperatures (T_g's) have been

https://dx.doi.org/10.1021/acssuschemeng.0c05364
ACS Sustainable Chem. Eng. 2020, 8, 16803−16813

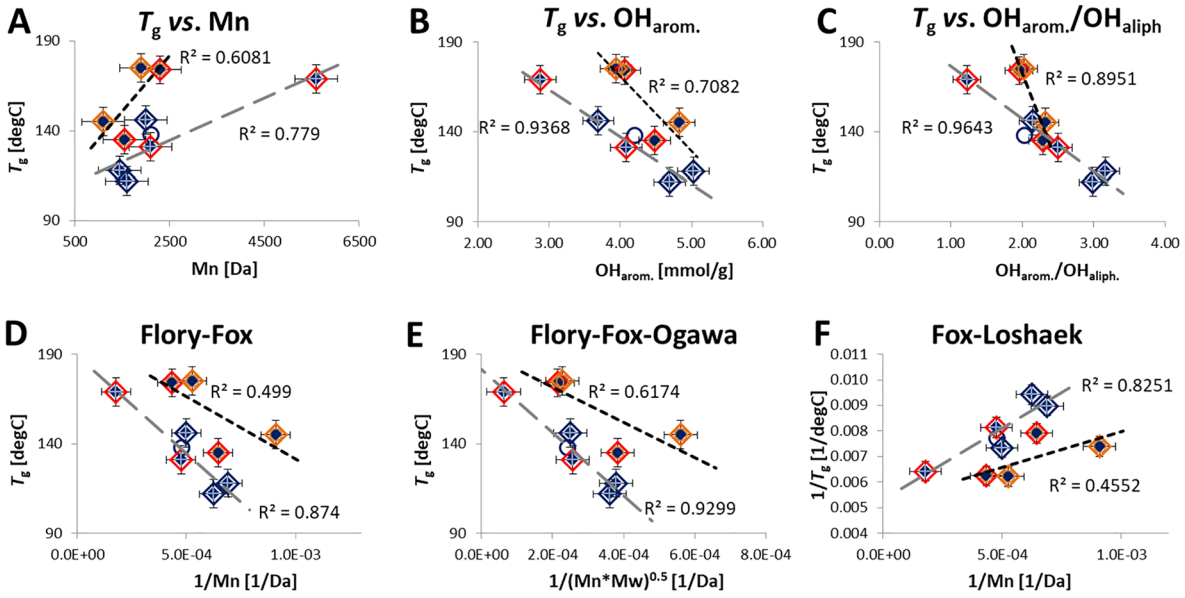

Figure 3. Correlation of glass transition temperatures with (A) the mean-average molecular weight (Mn), (B) the total amount of phenolic OH groups, and (C) the ratio between aromatic and aliphatic OH groups, as well as according to (D) Flory–Fox, (E) Flory–Fox–Ogawa, and (F) Fox–Loshaek theories. **SKL** parent kraft lignin is represented by the hollow circle, and pure acetone fractions are additionally evidenced by a blue rhomb, methanol–acetone fractions by a red rhomb, and pure methanol fractions by an orange rhomb. Lines represent regressions for identified regimes: black, smaller dashed line for methanol fractions with the exception of **MSAIKL-DB-SOX**; gray, larger dashed line for acetone fractions plus **MSAIKL-DB-SOX**.

plotted against (i) mean-average molecular weight, (ii) aromatic OH group content, and (iii) ratio between aromatic and aliphatic OH groups (Figure 3A–C). For testing whether molecular weight features would dominate T_g, irrespective of obviously important intra- and intermolecular H-bonding, T_g's were plotted also according to the following: (i) the classic Flory–Fox theory,[38] performing reliably for larger, rather narrowly polydispersed polymers; (ii) the Ogawa version of the Flory–Fox equation, developed for improved description of more polydispersed polymers;[39] and (iii) the Fox–Loshaek variation[40] that would indicate the major importance of cross-linking (Figure 3D–F).

Two regimes can be identified; within each regime, *i.e.*, within the fractions isolated by means of methanol and within the fractions delineated by means of acetone, the glass transition follows Mn. A rough but still uniform correlation in the investigated series of **SKL** fractions and their refinements is found for the glass transition temperature as a function of the ratio between aliphatic and aromatic OH groups (Figure 3C); correlating T_g to aromatic OH groups alone also shows similar trends across the same group of fractions. Generally, higher coefficients of determination are found for the simple correlations between the OH group content and T_g. Simple correlation between molecular weight features and T_g is weaker. When correlating molecular mass characteristics to T_g according to any of the aforementioned classical polymer theories, only the Flory–Fox–Ogawa model gives coefficients of determination (R^2) above 0.9. Glass transition temperatures thus underline also the importance of H-bonding as exerted by different types of OH groups and hence also the importance to eventually account for H-bonding characteristics during a fractionation approach to arrive at structural differences between fractions as much as possible, in addition to MW features.

CONCLUSIONS

SKL was fractionated using aprotic acetone and protic methanol to yield both traditional fractions and novel refined fractions based on differences in mutual H-bonding affinities exerted by the solvents on one side and the OH groups of the lignin on the other side. Sequential use of the two solvents practically resembled a refinement protocol that shed light on eventual "structural impurities" contained in the traditional fractions, which is not delineable easily in front of the background of a dominating spectroscopic image. "Structurally purified" lignin fractions in the form of condensed **ASKL** and **MSAIKL**, on the one hand, and polyphenylpropanoidic **MIAIKL**, on the other hand, allow for rather different types of value-adding applications while starting from a common low-cost technical lignin. If necessary, this refinement can be even more pronounced, adding a filtering step like the dialysis bags used in here in the fractional dissolution process, which allows filtering out of residues of "less degraded" oligomeric structures that pollute the simple **MSAIKL-SOX** fraction.

The original fractions and refined fractions generated based on targeting specific H-bonding affinities give a more homogeneous picture with respect to trends in glass transition temperatures, suggesting that T_g is dominated actually by MW and both the OH group amount and nature.

ASSOCIATED CONTENT

Supporting Information

The Supporting Information is available free of charge at https://pubs.acs.org/doi/10.1021/acssuschemeng.0c05364.

Images of the FT-IR and HSQC spectra of **SKL** and its fractions, as well as two tables indicating observed absolute and relative abundances of interunit bonding motifs obtained in the nonquantitative, standardized HSQC measurements (PDF)

https://dx.doi.org/10.1021/acssuschemeng.0c05364
ACS Sustainable Chem. Eng. 2020, 8, 16803–16813

AUTHOR INFORMATION

Corresponding Authors

Claudia Crestini − *Department of Molecular Science and Nanosystems, University of Venice Ca' Foscari, 30170 Venice Mestre, Italy; CSGI−Center for Colloid and Surface Science, 50019 Sesto Fiorentino, Italy;* orcid.org/0000-0001-9903-2675; Email: claudia.crestini@unive.it

Heiko Lange − *Department of Pharmacy, University of Naples 'Federico II', 80131 Naples, Italy; CSGI−Center for Colloid and Surface Science, 50019 Sesto Fiorentino, Italy;* orcid.org/0000-0003-3845-7017; Email: heiko.lange@unina.it

Authors

Reza Ebrahimi Majdar − *Department of Chemical Science and Technologies, University of Rome 'Tor Vergata', 00133 Rome, Italy*

Ali Ghasemian − *Department of Pulp and Paper Science and Technology, Gorgan University of Agricultural Sciences and Natural Resources, 4913815739 Gorgan, Iran*

Hossein Resalati − *Department of Wood and Paper Science and Industries, Sari University of Agricultural Sciences and Natural Resources, 4818168984 Sari, Iran*

Ahmadreza Saraeian − *Department of Pulp and Paper Science and Technology, Gorgan University of Agricultural Sciences and Natural Resources, 4913815739 Gorgan, Iran*

Complete contact information is available at: https://pubs.acs.org/10.1021/acssuschemeng.0c05364

Author Contributions

R.E.M. contributed to the investigation and writing and preparation of the original draft of the manuscript. A.G. was involved in the funding, supervision, and reviewing and editing of the manuscript. H.R. was involved in the supervision and reviewing and editing of the manuscript. A.S. contributed to the supervision and reviewing and editing of the manuscript. C.C. was involved in the funding, data curation, supervision, and reviewing and editing of the manuscript. H.L. contributed to the conceptualization, methodology, supervision, data curation, writing and preparation of the original draft of the manuscript, and reviewing and editing of the manuscript. All authors have given approval to the final version of the manuscript.

Notes

The authors declare no competing financial interest.

ACKNOWLEDGMENTS

R.E.M. would like to thank the Ministry of Science, Research and Technology of Iran, for the financial support. All authors would like to thank Stora Enso (Sunila Mill, Kotka, Finland) for providing LignoBoost softwood kraft lignin. Precious help with the thermal analyses by Mrs. Cadia D'Ottavi is gratefully acknowledged. H.L. acknowledges the MIUR grant 'Dipartimento di Eccellenza 2018-2022' to the Department of Pharmacy of the University of Naples 'Federico II'. C.C. acknowledges the Ca'Foscari FPI 2019 funding.

LIST OF ABBREVIATIONS

AIKL, acetone-insoluble kraft lignin; **ASKL**, acetone-soluble kraft lignin; DB, dialysis bag/tube; DMSO, dimethyl sulfoxide; DSC, differential scanning calorimetry; FT-IR, Fourier transform infrared; GPC, gel permeation chromatography; HSQC, heteronuclear single quantum coherence; **MIAIKL**, methanol-insoluble, acetone-insoluble kraft lignin; **MIKL**, methanol-insoluble kraft lignin; Mn, number-average molecular weight; **MSAIKL**, methanol-soluble, acetone-insoluble kraft lignin; **MSKL**, methanol-soluble kraft lignin; Mw, weight-average molecular weight; MW, molecular weight; NMR, nuclear magnetic resonance; PDA, polydiode array; PDI, polydispersity index; RI, refractive index; SOX, Soxhlet; **SKL**, softwood kraft lignin; T_g, glass transition temperature

REFERENCES

(1) Hu, T. Q. *Chemical Modification, Properties, and Usage of Lignin*; Kluver Academic/Plenum Publishers: New York, 2002.

(2) Glasser, W. G., Northey, R. A., Schultz, T. P., Eds. *Lignin: Historical, Biological, and Materials Perspectives*; ACS Symposium Series; American Chemical Society: Washington, DC, 1999; Vol. 742.

(3) Glasser, W. G.; Sarkanen, S. *Lignin: Properties and Materials*; ACS Symposium Series; American Chemical Society: Washington, DC, 1989.

(4) Argyropoulos, D. S. *Materials, Chemicals, and Energy from Forest Biomass*; ACS Symposium Series; American Chemical Society: Washington, DC, 2007.

(5) Lundquist, K.; Kirk, T. K. Fractionation-Purification of an Industrial Kraft Lignin. *Tappi* **1980**, *63*, 80−82.

(6) Schuerch, C. The Solvent Properties of Liquids and Their Relation to the Solubility, Swelling, Isolation and Fractionation of Lignin. *J. Am. Chem. Soc.* **1952**, *74*, 5061−5067.

(7) Gigli, M.; Crestini, C. Lignin Fractionation: Opportunities and Challenges. *Green Chem.* **2020**, *22*, 4722−4746.

(8) Sadeghifar, H.; Ragauskas, A. Perspective on Technical Lignin Fractionation. *ACS Sustainable Chem. Eng.* **2020**, *8*, 8086−8101.

(9) Cui, C.; Sun, R.; Argyropoulos, D. S. Fractional Precipitation of Softwood Kraft Lignin: Isolation of Narrow Fractions Common to a Variety of Lignins. *ACS Sustainable Chem. Eng.* **2014**, *2*, 959−968.

(10) Lange, H.; Schiffels, P.; Sette, M.; Sevastyanova, O.; Crestini, C. Fractional Precipitation of Wheat Straw Organosolv Lignin: Macroscopic Properties and Structural Insights. *ACS Sustainable Chem. Eng.* **2016**, *4*, 5136−5151.

(11) Lourençon, T. V.; Hansel, F. A.; da Silva, T. A.; Ramos, L. P.; de Muniz, G. I. B.; Magalhães, W. L. E. Hardwood and Softwood Kraft Lignins Fractionation by Simple Sequential Acid Precipitation. *Sep. Purif. Technol.* **2015**, *154*, 82−88.

(12) Saito, T.; Perkins, J. H.; Vautard, F.; Meyer, H. M.; Messman, J. M.; Tolnai, B.; Naskar, A. K. Methanol Fractionation of Softwood Kraft Lignin: Impact on the Lignin Properties. *ChemSusChem* **2014**, *7*, 221−228.

(13) Passoni, V.; Scarica, C.; Levi, M.; Turri, S.; Griffini, G. Fractionation of Industrial Softwood Kraft Lignin: Solvent Selection as a Tool for Tailored Material Properties. *ACS Sustainable Chem. Eng.* **2016**, *4*, 2232−2242.

(14) Hemmingson, J. A. Steam-Explosion Lignins: Fractionation, Composition, Structure and Extractives. *J. Wood Chem. Technol.* **1987**, *7*, 527−553.

(15) Duval, A.; Vilaplana, F.; Crestini, C.; Lawoko, M. Solvent Screening for the Fractionation of Industrial Kraft Lignin. *Holzforschung* **2015**, *70*, 11−20.

(16) Kim, J.-Y.; Park, S. Y.; Lee, J. H.; Choi, I.-G.; Choi, J. W. Sequential Solvent Fractionation of Lignin for Selective Production of Monoaromatics by Ru Catalyzed Ethanolysis. *RSC Adv.* **2017**, *7*, 53117−53125.

(17) Ebrahimi Majdar, R.; Ghasemian, A.; Resalati, H.; Saraeian, A.; Crestini, C.; Lange, H. Facile Isolation of LCC-Fraction from Organosolv Lignin by Simple Soxhlet Extraction. *Polymer* **2019**, *11*, 225.

(18) Majdar, R. E.; Crestini, C.; Lange, H. Lignin Fractionation in Segmented Continuous Flow. *ChemSusChem* **2020**, *13*, 4735−4742.

(19) Sevastyanova, O.; Helander, M.; Chowdhury, S.; Lange, H.; Wedin, H.; Zhang, L.; Ek, M.; Kadla, J. F.; Crestini, C.; Lindström, M.

E. Tailoring the Molecular and Thermo−Mechanical Properties of Kraft Lignin by Ultrafiltration. *J. Appl. Polym. Sci.* **2014**, *131*, 40799.
(20) Duval, A.; Molina-Boisseau, S.; Chirat, C. Fractionation of Lignosulfonates: Comparison of Ultrafiltration and Ethanol Solubility to Obtain a Set of Fractions with Distinct Properties. *Holzforschung* **2014**, *69*, 127−134.
(21) Dai, L.; Zhu, W.; Lu, J.; Kong, F.; Si, C.; Ni, Y. A Lignin-Containing Cellulose Hydrogel for Lignin Fractionation. *Green Chem.* **2019**, *21*, 5222−5230.
(22) Öhman, F.; Theliander, H.; Tomani, P.; Axegard, P. Method for Separating Lignin from Black Liquor. US8486224 B2, July 16, 2013.
(23) Crestini, C.; Lange, H.; Sette, M.; Argyropoulos, D. S. On the Structure of Softwood Kraft Lignin. *Green Chem.* **2017**, *19*, 4104−4121.
(24) Hansen, C. M. *Hansen Solubility Parameters : A User's Handbook, Second Edition*; *CRC Press*, 2007, DOI: 10.1201/9781420006834.
(25) Lange, H.; Rulli, F.; Crestini, C. Gel Permeation Chromatography in Determining Molecular Weights of Lignins: Critical Aspects Revisited for Improved Utility in the Development of Novel Materials. *ACS Sustainable Chem. Eng.* **2016**, *4*, 5167−5180.
(26) Granata, A.; Argyropoulos, D. S. 2-Chloro-4,4,5,5-Tetramethyl-1,3,2-Dioxaphospholane, a Reagent for the Accurate Determination of the Uncondensed and Condensed Phenolic Moieties in Lignins. *J. Agric. Food Chem.* **1995**, *43*, 1538−1544.
(27) Meng, X.; Crestini, C.; Ben, H.; Hao, N.; Pu, Y.; Ragauskas, A. J.; Argyropoulos, D. S. Determination of Hydroxyl Groups in Biorefinery Resources via Quantitative 31P NMR Spectroscopy. *Nat. Protoc.* **2019**, *14*, 2627−2647.
(28) Argyropoulos, D. S. 31P NMR in Wood Chemistry: A Review of Recent Progress. *Res. Chem. Intermed.* **1995**, *21*, 373−395.
(29) Prothmann, J.; Spégel, P.; Sandahl, M.; Turner, C. Identification of Lignin Oligomers in Kraft Lignin Using Ultra-High-Performance Liquid Chromatography/High-Resolution Multiple-Stage Tandem Mass Spectrometry (UHPLC/HRMSn). *Anal. Bioanal. Chem.* **2018**, *410*, 7803−7814.
(30) Lu, F.; Ralph, J. Derivatization Followed by Reductive Cleavage (DFRC Method), a New Method for Lignin Analysis: Protocol for Analysis of DFRC Monomers. *J. Agric. Food Chem.* **1997**, *45*, 2590−2592.
(31) S. Lancefield, C.; J. Wienk, H. L.; Boelens, R.; M. Weckhuysen, B.; A. Bruijnincx, P. C. Identification of a Diagnostic Structural Motif Reveals a New Reaction Intermediate and Condensation Pathway in Kraft Lignin Formation. *Chem. Sci.* **2018**, *9*, 6348−6360.
(32) Wen, J.-L.; Sun, S.-L.; Xue, B.-L.; Sun, R.-C. Recent Advances in Characterization of Lignin Polymer by Solution-State Nuclear Magnetic Resonance (NMR) Methodology. *Materials* **2013**, *6*, 359−391.
(33) Yuan, T.-Q.; Sun, S.-N.; Xu, F.; Sun, R.-C. Characterization of Lignin Structures and Lignin−Carbohydrate Complex (LCC) Linkages by Quantitative ^{13}C and 2D HSQC NMR Spectroscopy. *J. Agric. Food Chem.* **2011**, *59*, 10604−10614.
(34) Kubo, S.; Kadla, J. F. Hydrogen Bonding in Lignin: A Fourier Transform Infrared Model Compound Study. *Biomacromolecules* **2005**, *6*, 2815−2821.
(35) Perutz, M. F. The Role of Aromatic Rings as Hydrogen-Bond Acceptors in Molecular Recognition. *Philos. Trans. R. Soc. Lond. Math. Phys. Eng. Sci.* **1674**, *345*, 105−112.
(36) Giummarella, N.; Lindén, P. A.; Areskogh, D.; Lawoko, M. Fractional Profiling of Kraft Lignin Structure: Unravelling Insights on Lignin Reaction Mechanisms. *ACS Sustainable Chem. Eng.* **2020**, *8*, 1112−1120.
(37) Giummarella, N.; Pu, Y.; Ragauskas, A. J.; Lawoko, M. A Critical Review on the Analysis of Lignin Carbohydrate Bonds. *Green Chem.* **2019**, *21*, 1573−1595.
(38) Fox, T. G., Jr.; Flory, P. J. Second-Order Transition Temperatures and Related Properties of Polystyrene. I. Influence of Molecular Weight. *J. Appl. Phys.* **1950**, *21*, 581−591.
(39) Ogawa, T. Effects of Molecular Weight on Mechanical Properties of Polypropylene. *J. Appl. Polym. Sci.* **1992**, *44*, 1869−1871.
(40) Fox, T. G.; Loshaek, S. Influence of Molecular Weight and Degree of Crosslinking on the Specific Volume and Glass Temperature of Polymers. *J. Polym. Sci.* **1955**, *15*, 371−390.

https://dx.doi.org/10.1021/acssuschemeng.0c05364
ACS Sustainable Chem. Eng. 2020, 8, 16803−16813